UC San Diego
UC San Diego Electronic Theses and Dissertations

Title

Mutation of APP Caspase Cleavage Site at Position D664 Does Not Affect Dendritic Spine Morphology in Mice /

Permalink

https://escholarship.org/uc/item/5742z3n9

Author

Kawakatsu, Yusuke

Publication Date

2014

Peer reviewed|Thesis/dissertation

UNIVERSITY OF CALIFORNIA, SAN DIEGO

Mutation of APP Caspase Cleavage Site at Position D664 Does Not Affect Dendritic
Spine Morphology in Mice

A Thesis submitted in partial satisfaction of the requirements for the degree
Master of Science

in

Biology

by

Yusuke Kawakatsu

Committee in charge:

      Professor Edward Koo, Chair
      Professor Nicholas Spitzer, Co-Chair
      Professor Stefan Leutgeb

2014

The thesis of Yusuke Kawakatsu is approved and it is acceptable in quality and form for publication on microfilm and electronically

_____

_____
Co-Chair

_____
Chair

University of California, San Diego

2014

TABLE OF CONTENTS

LIST OF FIGURES

ACKNOWLEDGEMENTS

ABSTRACT OF THE THESIS

Mutation of APP Caspase Cleavage Site at Position D664 Does Not Affect Dendritic
Spine Morphology in Mice

by

Yusuke Kawakatsu

Master of Science in Biology

University of California, San Diego, 2014

Professor Edward Koo, Chair
Professor Nicholas Spitzer, Co-Chair

The amyloid cascade hypothesis posits that Alzheimer's disease (AD) is driven

by the production of Aβ from the cleavage of the amyloid precursor protein (APP) by

secretases. However, APP is also cleaved by caspases to release a toxic peptide termed

C31 into the cytoplasm that has been shown to increase cell death *in vitro*. A single

point mutation from Asp to Ala at position 664 of APP (APP695 numbering scheme)

prevents caspase cleavage of APP and attenuates Aβ-induced toxicity, demonstrating a

potential role for caspase cleavage of APP in Alzheimer's pathology. However, due to disadvantages such as APP overexpression and insertional artifacts in some transgenic lines, the protective effect of the D664A mutation remains unclear. We have developed a knock-in mouse line carrying the D664A mutation to study its effects on baseline dendritic morphology by crossing it with the GFP-M mouse. Immunofluorescent staining of DA/GFP-M brain sections revealed that the D664A mutation itself had no impact on the basal or apical dendritic spine morphology when compared to their WT/GFP-M littermates across different age groups. In a second study, primary hippocampal neuronal cultures from the DA mice and their WT littermates were treated with 7PA2 conditioned media (7PA2-CM) containing various Aβ42 concentrations of to quantify the protective effect of this D664A mutation in dendritic spine density. However, our neuronal culture experiments failed to demonstrate any protective effects of the D664A mutation as it was retrospectively discovered that our 7PA2-CM lacked the Aβ42 oligomers necessary to induce toxicity in WT controls.

INTRODUCTION

Alzheimer's disease

Alzheimer's disease (AD) is the most common form of neurodegenerative disease and cause of dementia in the United States. Based on linear extrapolation from published prevalence estimates for 2010, it is believed that currently in the year 2014 there are 5.2 million older Americans over the age of 65 affected by AD in the United States (Hebert et al., 2013). Starting with a gradual loss in ability to retain new information, individuals affected by AD show symptoms including confusion, loss of memory that disrupts daily life, trouble speaking or writing, decreased or poor judgment, and severe changes in mood and personality (Alzheimer's Association, 2014). AD is fatal and will lead to death in 8 to 10 years from diagnosis. To this day, a complete understanding of the disease' underlying mechanisms is still lacking and there is no known way to prevent, delay, or cure the disease. Although there are drugs for AD approved by the FDA such as acetylcholineresterase inhibitors and NMDA antagonists, they only mildly alleviate symptoms and have no effect on disease progression (Blennow et al., 2006). With anticipated increase in life expectancy and those of the baby boom generation growing older, the number of people diagnosed with AD is expected to increase to anywhere from 11 million to 16 million by the year 2050 (Hebert et al., 2013). The cost of care for AD patients in the United States for 2014 is estimated to be approximately $214 billion, not including unpaid care by

1

relatives and friends of patients (Alzheimer's Association, 2014). This cost is estimated to increase to $1.2 trillion by 2050.

Pathological Hallmarks of Alzheimer's Disease

The two pathological hallmarks of AD are extracellular amyloid plaques and intracellular neurofibrillary tangles (Figure 1). Extracellular plaques are composed of β-amyloid peptides (Aβ) released from the extracellular domain of the β-amyloid precursor protein (APP). APP is a transmembrane protein that has been suggested to function as a receptor or a ligand for its capabilities to interact with various molecules such as Aβ, F-spondin, Nogo-66 receptor, and Netrin-1 and these interactions have shown to affect Aβ production *in vitro* (Lorenzo et al., 2000, Ho and Sudhof, 2004, Park et al., 2006, Lourenco et al., 2009). APP also regulates NMDA receptor function, synaptic plasticity and spatial memory while reduction or loss of APP is associated with impaired neurite outgrowth and neuronal viability *in vitro* and synaptic activity *in vivo* (Taylor et al., 2008, Allinquant et al., 1995, Perez et al., 1997, Herard et al., 2006). Alternate splicing of APP creates three distinct protein species of different sizes, which are APP695, APP751, and APP771 with APP695 being the predominant form expressed in neurons in the brain (Sisodia et al., 1993).

APP is primarily cleaved by α-secretase to yield extracellular APPsα and then subsequently have the remaining α-carboxyl-terminal fragment (APP-CTFα) cleaved by γ-secretase to release p3 from its extracellular domain, leaving behind the APP intracellular domain (AICD) inside the cell (Figure 2). In the amyloidegenic pathway,

APP is cleaved by β-secretase to release APPsβ and the remaining APP-CTFβ is cleaved by γ-secretase to release Aβ peptide into the lumen (Zheng and Koo, 2011). Aβ peptides accumulate and aggregate to become the main constituent of the amyloid plaques seen in AD patients. Aβ42 is known to be the more toxic of the Aβ species as it is longer and more hydrophobic relative to Aβ40, making it more prone for extracellular aggregation (Selkoe, 2001).

Neurofibrillary tangles, the second hallmark of AD, are composed of hyperphosphorylated tau protein. Tau is a soluble axonal protein that binds tubulin and promotes microtubule assembly and stability in neurons of the central nervous system. These tau proteins have six different isoforms resulting from alternative splicing of the microtubule-associated protein tau gene (Goedert et al., 1988). Phosphorylation of tau leads to tau binding to microtubules and disrupting microtubule organization, which at normal levels is required for controlling microtubule stability in a neuron. When tau is abnormally hyperphosphorylated, it sequesters normal tau proteins in paired helical filaments that form neurofibrillary tangles containing all six isoforms (Iqbal et al., 2005). This eventually leads to neuron degeneration in retrograde manner in which proper microtubule regulation is compromised and neurons lose the ability to carry out proper intracellular transportation of functional proteins across axons due to aggregation of tau protein in tangles (Wang et al., 2013). Tau pathology is observed in other forms of dementia as well such as Parkinson's disease where the hyperphosphorylated form of tau leads to neurofibrillary degeneration.
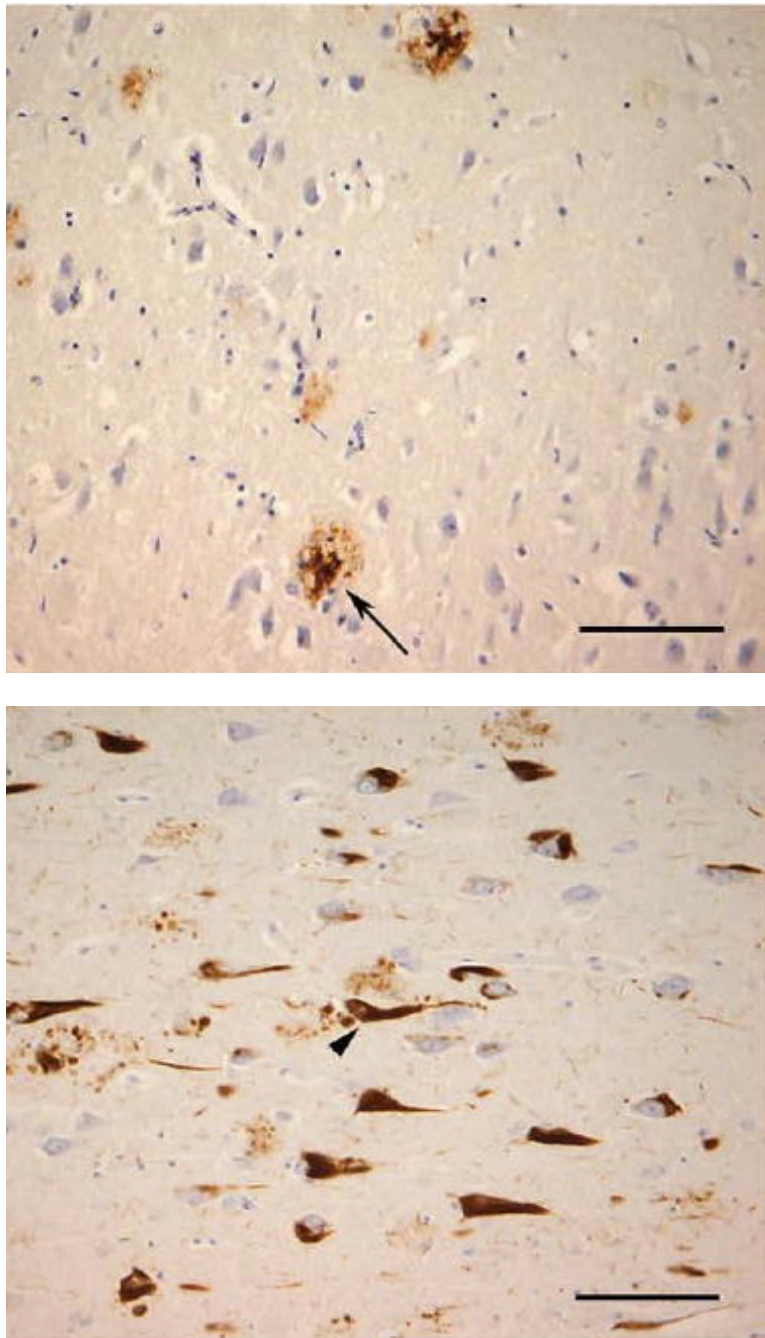
Figure 1. Amyloid plaques and neurofibrillary tangles

A modified Bielschowky's silver staining showing amyloid plaques (top image arrow) and neurofibrillary tangles (bottom image arrowhead). Scale bars = 120 μm. This image is adapted from Purohit et al., 2011.

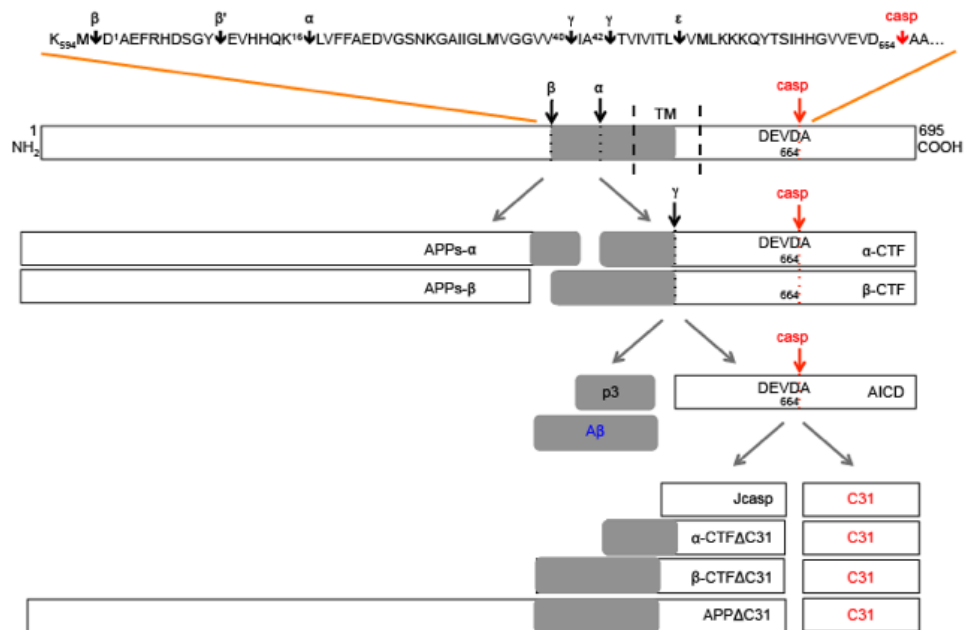Figure 2. Schematic for APP processing

Diagram showing the various cleavage events of APP by different secretases and caspases.

Genetics of Alzheimer's Disease

Cases of familial Alzheimer's disease (FAD) have been extensively studied in an attempt to improve understanding of the genetic basis of AD. Studies have found that mutations in APP, presenilin-1 (PSEN1), and presenilin-2 (PSEN2) genes lead to an earlier onset of the disease with aggressive disease progression in patients under the age of 65 (Goate et al., 1991, Harvey et al., 2003). The presenilin proteins are transmembrane proteins that, along with nicastrin, anterior pharynx defective (APH1), and presenilin enhancer (PEN2), make up γ-secretase. Together with β-secretase, they cleave APP to release the toxic Aβ peptide (Iwatsubo, 2004). Findings on these FAD mutations provided initial insights in the link between Aβ accumulation and AD, as all FAD mutations affect processing of APP. FAD mutations either induce higher total Aβ production by favoring β-secretase cleavage of APP over α-secretase cleavage or they selectively increase Aβ42 production over Aβ40 (Hardy and Selkoe, 2002, Tanzi and Bertram, 2005).

FAD accounts for only approximately 1% of all cases of AD and the remainder of all cases are sporadic in origin and typically occur in the elderly over the age of 65 (Alzheimer's Association, 2012). There are no known definitive causes of sporadic AD, but studies have shown many risk factors associated with the disease. A significant risk factor for sporadic AD is carrying the Apolipoprotein E (ApoE) ε4 allele. Carrying one copy of the ApoE ε4 allele increases the likelihood of developing sporadic AD by 2 to 3 fold while carrying two copies increases chances by 12 fold (Corder et al., 1993, Strittmatter et al., 1993). It has been suggested that ApoE

functions to enhance proteolytic break-down of Aβ within and outside of neurons and that the ε4 isoform of ApoE is not as efficient as other isoforms in enhancing these reactions and thus carries with it a risk for AD in the elderly (Jiang et al., 2008). If an individual has one or more primary relatives with AD, the individual would have a significantly higher chance of developing AD as they may be sharing genetic and lifestyle factors that contribute to AD (Mayeux et al., 1991). Other risk factors include aging, smoking, obesity, alcohol consumption, lack of education, head injuries, diabetes, and various environmental factors (Yaffe et al., 2001, Chen et al., 2009). It is generally accepted that AD is caused by a combination of various factors and it is even speculated that brain changes leading to AD are brought upon by such factors as many as 20 years before symptoms show making it difficult to pinpoint a single definitive cause.

Amyloid Cascade Hypothesis

The amyloid cascade hypothesis, which has played a prominent role in guiding AD research, posits that the extracellular release of Aβ peptide from the processing of APP by β-secretase and γ-secretase is what drives disease progression in AD. The neurofibrillary tangles, cell loss, vascular damage, and dementia are results of this extracellular Aβ deposition according to the amyloid cascade hypothesis (Hardy and Higgins, 1992). This hypothesis is supported by the facts that the Aβ peptide is the main component of amyloid plaques found in AD patients and large quantities of Aβ are toxic to cells *in vitro* (Glenner and Wong, 1984, Goodman and Mattson, 1994).

Autopsied AD brains have confirmed that formation of Aβ plaques precede the formation of neurofibrillary tangles (Hardy and Selkoe, 2002). The hypothesis is also consistent with observations in which mutations that induce FAD increase the ratio of the toxic Aβ42 to Aβ40 in the brain (Tanzi and Bertram, 2005). However it remains unclear as to what causes the initial increase in production of Aβ in patients with sporadic AD who do not carry such mutations.

Aβ-induced Synaptotoxicity and Synapse Loss

Aβ deposition leads to the formation of Aβ plaques, but increased levels of insoluble Aβ plaque in human brains have not shown a strong correlation with cognitive alterations or dementia (Price et al., 2009). Research has shown that instead of the insoluble Aβ plaques, it is the soluble Aβ species that cause synaptic damage (Shankar et al., 2007). When the Aβ peptide is released from APP at the cell membrane it is initially in a soluble monomeric form that then interacts with other Aβ peptides to form higher molecular weight soluble oligomers. Various *in vitro* studies suggest that it is these soluble Aβ oligomers that are the cause of neurotoxicity leading to cognitive alterations and dementia in AD patients (Shankar et al., 2007). One such study by Shankar and colleagues demonstrated that rat organotypic brain slice cultures treated with soluble Aβ monomers were indistinguishable from control samples in terms of dendritic spine density (an indicator of synaptic health), while samples treated with low-n soluble oligomers of Aβ had dendritic spine density levels that were four-

fold less than control levels (Shankar et al., 2007). These results showed that soluble low-n Aβ oligomers trigger synapse loss and that the soluble Aβ monomers alone do not carry the same neurotoxic effects. However, it remains unclear how the presence of soluble low-n Aβ oligomers induces loss of synaptic function in neurons.

Caspase Cleavage of APP at D664 and the D664A mutation

Apart from its amyloidegenic pathway involving secretases, APP is also cleaved at its C-terminal by caspases or caspase-like proteases (Figure 2). When APP is cleaved by caspases at position D664, a peptide containing the last 31 amino acids of APP at its C-terminal is released into the cytoplasm (Weidemann et al., 1999). When this peptide, termed C31, is expressed in N2a mouse neuroblastoma cells, it dramatically increases cell death, demonstrating its toxic properties and its potential to be involved in Aβ toxicity (Lu et al., 2000). A single point mutation at position 664 of APP from aspartic acid to alanine completely prevents cleavage of APP at this position by caspases and thus prevents the release of C31 into the cell (Lu et al., 2000). This D664A mutation (referred simply as DA in this thesis) in APP has shown to be sufficient to attenuate Aβ toxicity and significantly decrease cell death in N2a cells and B103 rat neuroblastoma cells from Aβ treatment down to control levels (Lu et al., 2003). Together these findings show that the generation of C31 at position D664 or the presence of caspase at that location is one possible pathway in mediating Aβ toxicity. It is important to note that the DA mutation has no effect on Aβ production and only prevents the toxic effects of Aβ from inducing cell death (Soriano et al.,

2001). Lu and colleagues provided further evidence for the role of C31 in Aβ toxicity by demonstrating the dependence of both C31 and the Aβ peptide on the presence of APP in the cell. In cell culture, B103 and N2a cells only treated with Aβ or only expressing C31 had cell death rates that were indistinguishable from control samples while samples with APP overexpression and Aβ treatment and samples co-expressing APP and C31 had cell death rates that were four-fold and three-fold greater than control samples, respectively (Lu et al., 2003). This finding strongly suggests that the two toxic peptides function in pathways related to one another. The mechanisms of C31 toxicity are not well understood, but it has been observed that AICD, which contains the last 31 amino acids of APP that make up C31, can translocate into the nucleus and modulate gene expression by interacting with Fe65 (Cao and Sudhof, 2001, Baek et al., 2002). Therefore it is possible that the C31 peptide enters the nucleus once it is released from APP and acts as a transcription factor that initiates a cell death pathway (Kinoshita et al., 2002).

Behavioral studies carried out in mice have also demonstrated the protective effects of the DA mutation from behavioral abnormalities. In 2006 Saganich and colleagues tested J20 mice with APP overexpression and B21 mice with APP overexpression carrying the DA mutation in the Morris Water Maze (MWM) by measuring the distance traveled by the mice attempting to find a hidden platform just below the surface of the water. There was no significant difference in performance between transgenic and non-transgenic mice that were 3-4 months old, but in older mice that were 8-12 months old it was observed that J20 mice took significantly

longer to find the hidden platform compared to non-transgenic littermates while B21 mice carrying the DA mutation had performances that were comparable to non-transgenic littermates (Saganich et al., 2006). Other studies have also shown that mice carrying the DA mutation had no significant learning deficiencies in the MWM and exhibited normal morphological characteristics compared to control transgenic mice not carrying the DA mutation despite heavy Aβ plaque and soluble Aβ burden in their brains (Galvan et al., 2006, Zhang et al., 2010).

Similar results displaying the protective effect of the DA mutation were observed in electrophysiological recording from cultured organotypic hippocampal slice culture where overexpression of CT100 carrying the DA mutation could blunt the Aβ-mediated synaptic depression and prevent loss of AMPAR- or NMDAR-mediated currents (Midthune et al., 2011).

Although these previous findings are strongly indicative of the protective effects of the DA mutation from Aβ toxicity and subsequent behavioral abnormalities, it is difficult to exactly quantify this protective effect. Up to this point all mouse models used to study the effects of the DA mutation have relied on APP or C31 overexpression to drive amyloid pathology, which does not accurately reflect the nature of AD *in vivo*. Due to the uncertain amount of negative effects caused by APP overexpression, it is unclear as to how much of this negative effect is alleviated by the DA mutation. It is also unclear if mice carrying the DA mutation start with healthier brains than wild-type mice and are then damaged by APP overexpression or the protective effect of the DA mutation takes effect after APP overexpression by

reducing the amount of damage. For certain transgenic mouse models there have also been undesired phenotypes observed such as the one described in the behavioral study carried out by the Zhang group where young B254 mice showed a phenotype similar to the tonic phase of a seizure when exposed to the MWM (Zhang et al., 2010). It is unclear if such phenotypes are caused by the DA mutation, APP overexpression, or another factor altogether.

Also, *in vivo* results from those lines of DA transgenic animals have been inconsistent, and did not clarify the DA mutation's effects *in vivo*, mostly because the substitution was done in transgenic animals that were already engineered to overexpress APP. A subsequent re-examination of a high expressing DA transgenic mouse line failed to reproduce the initial findings (Harris et al., 2010). Further, the *in vivo* therapeutic effects of that mutation seem to diminish in older animals (Galvan 2006, Zhang 2010). More importantly, this transgenic model did not "reverse" any existing pathology in the animals as claimed by those papers; rather, the mouse lines showed the absence of anticipated pathology. Thus, one cannot be certain that the lack of these predicted amyloid-associated alterations was due to loss of the caspase cleavage and not to insertional artifact, random mutation, or other unanticipated and undesirable effects of over-expression, etc. The only approach that can address this concern directly is to use a knock-in strategy where we can compare wild type and knock-in animals in which the only change is a base substitution (from D to A) to abrogate caspase mediated cleavage of APP. Therefore, a careful study of the APP DA knock-in mice will inform us whether this APP cytoplasmic domain mediate APP-

dependent synaptotoxicity leads to neuronal death, and whether this mechanism is common to both normal aging and the generation of AD pathology.

Specific Aims

The first aim of this project is to examine whether the DA mutation itself has an effect on neuronal dendritic spine morphology in the DA mouse. DA mice were crossed with an established GFP-M mouse line that expresses GFP in neurons to produce DA/GFP-M mice, which will allow us to study and characterize neuron morphology through fluorescent microscopy. We hypothesize that these DA/GFP-M mice would have positive to neutral influence on neuronal morphology in terms of dendritic spine density compared to WT/GFP-M mice without the DA mutation, since previous studies have only shown absence of AD pathology in mice carrying the DA mutation even when the system is challenged by APP overexpression.

The second aim of this project is to quantify the protective effect of the DA mutation in hippocampal neuronal cultures for $A\beta$ toxicity. DA primary hippocampal neuronal cultures transiently transfected with GFP will be treated with 7PA2-CM with varying concentrations of $A\beta42$ to see if the DA mutation can successfully attenuate $A\beta$ toxicity compared to the neurons from WT neuronal cultures not carrying the DA mutation. This will also be analyzed in terms of dendritic spine density. It is expected for the DA neurons to have significantly higher dendritic spine density compared to WT littermates after $A\beta$ treatment.

Results from these experiments could provide us with a better understanding of the extent to which the DA mutation attenuates Aβ toxicity and the extent to which APP cleavage and C31 release from APP is required for spine loss and subsequent loss of neuronal synaptic function.

MATERIALS AND METHODS

The D664A mice

A heterozygous mouse carrying the DA mutation and a neomycin (neo) selection cassette flanked by the FRT sequences was obtained from Ingenious Targeting Laboratory. That heterozygous mouse was crossed with the B6.129S4-*Gt(ROSA)26Sor^{tm2(FLP*)Sor}*/J mouse (The Jackson Laboratory) to remove the neo cassette, then back crossed with a wild-type C57BL/6J mouse to remove the Flp recombinase gene in its genome. Heterozygous DA mice carrying only the D664A mutation in the C57BL/6J background were mated with its heterozygous littermates to obtain homozygous offsprings.

Genotyping D664A mice

DNA Extraction

DNA for genotyping was collected from toes or tails of mice. Toes or tails were digested in 500 μl of tail lysis buffer consisting of 100 mM Tris-HCl (pH 8-8.5), 5 mM EDTA, 0.2% SDS, and 200 mM NaCl with 3 μl of proteinase K added. The mixture was incubated for ~5 hours in a water bath at 55°C with agitation by vortex every 30 minutes. The mixture was then centrifuged at 14,000 rpm for 10 minutes. The supernatant was added to 300 μl of isopropanol and the DNA was collected on a pipette tip. The DNA was then dissolved in 150 μl of TE buffer consisting of 10 mM Tris-HCl (pH 8-8.5) and 0.1 mM EDTA in deionized water.

Polymerase Chain Reaction

To confirm the absence of the neomycin selection cassette in the DA mice, 1 µl of dissolved DNA in TE buffer was added to 12.5 µl of 2x DreamTaq Green PCR Master Mix (Thermo Scientific), 9.5 µl of deionized water, 1 µl of forward primer (GCA TCG CCT TCT ATC GCC TTC TTG), and 1 µl of reverse primer (GGG GAT GCT TCT TGT GAA CG). The PCR protocol consisted of 5 minutes at 99°C and 35 repeats of 30 seconds at 95 °C, 1 minute at 58°C, and 1 minute at 72°C with a final holding temperature of 4°C. Gel electrophoresis was carried out on PCR products on a 1% agarose gel with ethidium bromide (Apex) and if the neomycin selection cassette was present it would show as a band of 886 bp.

To confirm the absence of the Flp recombinase transgene, 1 µl of dissolved DNA in TE buffer was added to 12.5 µl of 2x DreamTaq Green PCR Master Mix, 9.5 µl of deionized water, 1 µl of each forward primer (GCA CTT GCT CTC CCA AAG TC and CTT TAA GCC TGC CCA GAA GA), and 1 µl of each reverse primer (GGG CGT ACT TGG CAT ATG AT and GCG AAG AGT TTG TCC TCA ACC). The PCR protocol consisted of 7 minutes at 94°C, 45 seconds at 94°C, 30 seconds at 58°C, 1 minutes at 72°C, 35 repeats of step 2 to 4, with an additional 10 minutes at 72°C at the end of 35 repeats with a final holding temperature of 4°C. If the Flp recombinase transgene was present it would show up as a band of 330 bp, else 252 bp

To detect the presence of the DA mutation in the APP gene, 1 µl of dissolved DNA in TE buffer was added to 12.5 µl of 2x DreamTaq Green PCR Master Mix, 9.5 µl deionized water, 1 µl of forward primer (TG CTT TCT AGG TCG CT), and 1 µl of

reverse primer (ATG AAC ACC GAT GGG TAG TGA AGC). The PCR protocol consisted of 5 minutes at 95°C, 35 repeats of 30 seconds at 95°C, 1 minute at 58.5°C, and 30 seconds at 72°C with an additional 2 minutes at 72°C at the end of 35 repeats with a final holding temperature of 4°C. If the DA mutation was present it would show as a band of 191 bp (Figure 3). The same protocol was carried out with a different forward primer (TG CTT TCT AGG TCG AC) and the same reverse primer to detect the presence of the WT APP gene. The presence of WT APP gene would show as a band of 191 bp. This was done to determine if the animal was WT for the APP gene, homozygous for the DA mutation, or heterozygous for the DA mutation.
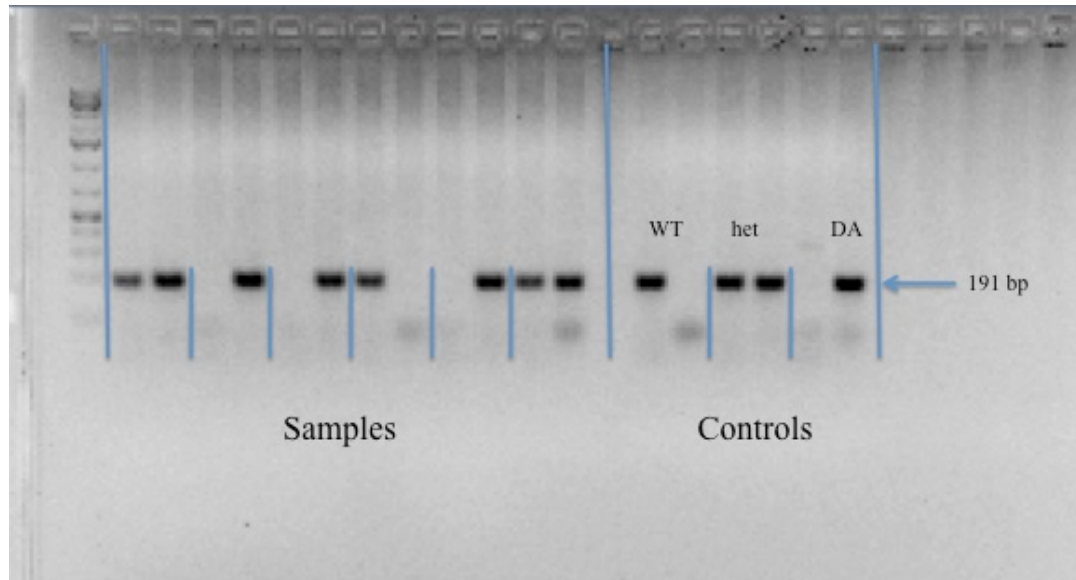
Figure 3. Genotyping for detection of the DA mutation

Extracted DNA from DA/GFP-M mice underwent two separate PCR reactions with one using primers to detect the presence of WT APP allele and another reaction using primers to detect the presence of DA APP allele. The two reactions for the same animal are run next to each other with the reaction detecting WT APP allele on the left and the reaction detecting DA APP allele adjacent to it on the right. Both reactions produce a PCR product at 191 bp.

DA/GFP-M mice

For immunofluorescent staining experiments, DA mice used for neuronal culture experiments were crossed with GFP-M mice to produce mice that were heterozygous for the DA mutation and heterozygous for GFP. Mice heterozygous for both genes were crossed with each other to produce DA homozygotes and WT littermates that were also GFP heterozygotes for the study.

Genotyping DA/GFP-M mice

To detect the presence of the GFP transgene 1 μl of dissolved DNA in TE buffer was added to 12.5 μl of 2x DreamTaq Green PCR Master Mix, 9.5 μl deionized water, 1 μl of forward primer (AAG TTC ATC TGC ACC ACC G), and 1 μl of reverse primer (TCC TTG AAG ATG GTG CG). The PCR protocol consisted of 90 seconds at 94°C, 35 repeats of 30 seconds at 94°C, 1 minute at 58°C, and 30 seconds at 72°C with an additional 2 minutes at 72°C at the end of 35 repeats with a final holding temperature of 4°C. The presence of the GFP transgene would show as a band of 173 bp (Figure 4). Real-Time PCR was carried out by the UCSD CORE facility to determine if animals positive with the 173 bp band were carrying 1 or 2 copies of the GFP transgene.
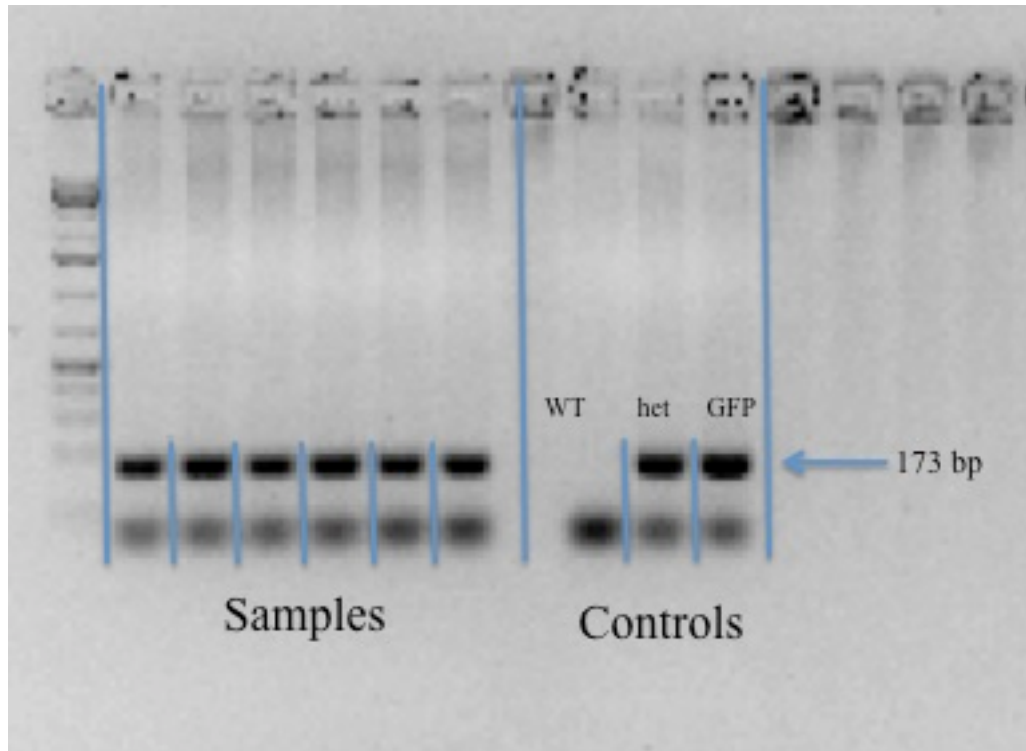
Figure 4. Genotyping for detection of the GFP transgene

Samples showing a band at 173 bp are either heterozygous or homozygous for the GFP transgene. qPCR was later carried out to determine if these samples were carrying one or two copies of the GFP transgene.

Perfusion and preparing brain sections for staining

Six to 12 months old DA/GFP-M mice were anesthetized with isoflurane and perfused with 100 mL cold 4% PFA in 1x PBS. Brains were then removed and stored in 4% PFA overnight at 4°C. After overnight fixation in 4% PFA, brains were stored in 30% sucrose in 1x PBS at 4°C until sucrose permeates the entire brain, which is about a week. A freezing microtome (Microm HM 400) was used to prepare 50 μm-thick whole brain sections. The cerebellum was removed and the brain was mounted on the stage. Dry ice was added to wells on both sides of the stage to freeze the brain. Brain sections were collected serially in a 24-well plate and stored in 1x PBS in darkness until GFP immunofluorescent staining.

GFP immunofluorescent staining

GFP immunofluorescent staining on mice brain sections was carried out free-floating using a 24 flat-bottom multi-well culture plate (PELCO) fitted into a 24-well culture plate (Greiner Bio-One) with 6 brain sections in each well. Brain sections were blocked for 1 hour at RT in blocking buffer consisting of 5% normal donkey serum (NDS) (Jackson ImmunoResearch), 2% BSA, and 0.25% Triton X in 1x PBS. Sections were then incubated in chicken anti-GFP primary antibody (Aves Lab) at about 400μl, 10mg IgY/ml, in blocking buffer for 2 hours at RT. After 2 quick washes with PBS, sections were washed 5 times (for 3 minutes each) with working buffer (10% blocking buffer, 90% of 0.1% Triton X in 1x PBS) and incubated in AlexaFluor 488-conjugated donkey anti-chicken secondary antibody (LifeTechnologies) at 1:750 dilution in

blocking buffer for 1 hour in darkness at RT. Sections were washed twice quickly with

PBS, washed 5 times (for 3 minutes each) with 0.1% Triton X in 1x PBS and then

counterstained with 10μM DAPI for 10 minutes. Sections were washed 5 times (for 3

minutes each) with PBS and mounted on microscope slides and dried overnight in

darkness. Mounted sections on slides were dehydrated by successive washes in 50% (3

minutes), 70% (3 minutes), 95% (3 minutes), and 100% ethanol (10 minutes) followed

by two washes in xylene (1 and 15 minutes respectively). Coverslips were placed on

slides with Harleco's Krystalon mounting medium (Millipore).

Image acquisition and spine quantification in immunofluorescent stained sections

GFP immunofluorescent-stained sections were imaged on the Olympus DSU

IX-81 inverted microscope at 60x/1.2 N.A. water immersion objective. For each

animal 6 neurons were selected randomly from the CA1 region for imaging. Dendritic

segments selected for analysis had to fulfill the following criteria: 1) the selected

segment must be at least 50-μm away from the cell body; 2) the selected segment must

be after the first branch point of the dendrite; and 3) the selected segment must not be

at the ending tip of the dendrite. Additionally dendritic segments were selected such

that no other segments overlapped with each other in a way that would obscure

visualization of spines. Dendritic spine density was scored from 3 basal dendritic

segments and 3 apical dendritic segments. Z-sections were taken at 0.2-μm intervals.

All imaging and analyses of dendritic spine density was carried out blind to genotype.

Dendritic spine density was acquired manually through the use of the Slidebook program and ImagePro 6.2.

7PA2-conditioned medium

7PA2 cells carrying the FAD mutation V717F in APP were grown to near confluence in 10% fetal bovine serum (FBS) (Omega) in 1x Dulbecco's Modified Eagle Medium (DMEM) (Corning Cellgro). Cells were washed twice with 1x phosphate-buffered saline (PBS) and were conditioned with plain 1x DMEM for 16 hours. The 7PA2-conditioned medium (7PA2-CM) was cleared of cells via centrifugation at 1000 rpm for 10 minutes. The 7PA2-CM was then concentrated ~10-fold by using YM-3 Centriprep filters (Millipore) and centrifugation at 3000 rpm for 20-25 minutes. This was repeated once or twice at shorter runs of ~10 minutes until the volume of the 7PA2-CM was reduced 10-fold. The 7PA2-CM was aliquoted and kept at -80°C.

Aβ40, 42 sandwich ELISA

ELISA plates (Immulon) were coated with 100 mL/well of Ab9 antibody to detect Aβ 1-40 or MM26.2.1.3 (Dr. Todd Golde, University of Florida) to detect Aβ 1-42 at 50 μg/mL in 1x PBS. Plates were covered with sealing tape and kept at 4°C overnight. The next day solution was discarded from plates and 200 μl of 1% block ACE (Serotec) in 1x PBS was added to each of the wells. The plates were covered with sealing tape and kept at 4°C overnight. The next day wells were washed twice

with 200 μl 1x PBS. 50 μl of ELISA coating buffer (EC) (0.4 M NaCl, 2mM EDTA, 0.2% block ACE, 0.2% bovine serum albumin (BSA), 0.05% CHAPS, and 0.05% NaN in 1x PBS) was added to each well. 100 μl samples of 7PA2-CM were added to duplicate wells while 100 μl standard controls were also prepared in duplicate wells at concentrations of 200, 100, 50, 25, 12.5, and 0 pM. The plates were covered and kept at 4°C overnight. The next day plates were washed with 200 μl 1x PBS. Each well coated with Ab9 was treated with 100 μl of HRP-conjugated 13.1.1 antibody (1:1000 dilution from a 1 mg/mL stock) in buffer C containing 1% BSA in 1x PBS. Each well coated with MM26.2.1.3 was treated with 100 μl of HRP-conjugated 6E10 antibody (1:1000 dilution from a 1 mg/mL stock) in buffer C. Plates were sealed and incubated for 4 hours at room temperature (RT). Wells were washed 3 times with 200 μl 0.5% Tween in 1x PBS (PBST) followed by 2 washed with 200 μl 1x PBS. Wells were then treated with 100 μl of pre-warmed (RT) 1-Step Ultra TMB ELISA (Serotec). Upon seeing color development in 200, 100, and 50 pM controls 100 μl of 2M H_2SO_4/PBS was added to each well. Colormetric analysis was carried out at λ450 nm. All ELISA experiments in this report were carried out by Hiroko Maruyama.

Western Blot of 7PA2-CM

7PA2-CM samples were diluted with 4X NuPAGE LDS sample buffer (Invitrogen) and boiled at 70°C for 7 minutes. The resolving gel prepared was 16% Bis-Tris buffer (pH 6.4). Samples were run with 1x MES SDS running buffer at 120 mV. The protein samples were transferred from the gel to a nitrocellulose membrane

immersed in 1x transfer buffer consisting of Tris-Glycine transfer buffer and methanol in deionized water at 300-400 mA for 1 hour at 4°C. Nitrocellulose membrane was washed with water and then blocked for 1 hour with 5% skim milk in 1x TBS with 0.1% Tween detergent (TBS-T). The membrane was washed thrice with TBS-T (5 minutes each) and then treated with 6E10 primary antibody (1μg/ml) for an hour, then washed thrice with TBS-T (5 minutes each) and detected with horse radish peroxidase conjugated anti-mouse secondary antibody. Membrane was developed using SuperSignal West Pico Chemiluminescent Substrates (Thermo Scientific) and HyBlot CL® Autoradiography Film (Denville). All Western blot experiments in this report were carried out by Floyd Sarsoza.

Hippocampal culture and transfection

Pre-treat coverslips:

12mm coverslips (Fisherbrand) were cleaned in 70% ethanol for 20 minutes and then washed 3 times (for 5 minutes each) with autoclaved deionized water. Individual coverslips were then placed into a 24-well plate and dried using a pipette. 350 μl of 30 μg/ml poly-L-lysine (Sigma) (in borate buffer, 0.15 M, pH 8.4) was placed in each well and allowed to incubate overnight at 37°C. The following day coverslips were washed briefly 3 times with water and then dried completely. The 24-well plate was covered in parafilm and kept at 4°C. Before dissection of pups, 500 μl of 1x DMEM was placed in each well to cover coverslips and the plate was kept at 37°C until neurons were ready to be plated.

Culture:

Primary hippocampal neurons were cultured from P0 to P1 pups from DA+/-
parents. Brains were removed from each pup and placed in cold wash buffer
consisting of 10 mM glucose and 100 units/ml penicillin 100 µg/ml streptomycin
(Pen/Strep) (Gibco) in 1x Ca^{2+}/Mg^{2+} free Hanks Balanced Salt Solution (HBSS)
(Invitrogen). 2 hippocampi were collected from each brain and the tail was collected
for genotyping. Individual hippocampi from each pup were dissected and processed
separately. Dissected hippocampi were washed briefly 3 times with 5 ml wash buffer.
The supernatant was discarded and each hippocampus was treated with 2.5 ml of
.125% Trypsin solution (Gibco) in HBSS pre-warmed at 37°C. Hippocampi were then
incubated in a 37°C water bath for 20 minutes with occasional stirring. 250 µl of FBS
stock was added to each sample and centrifuged for 5 minutes at 2000 rpm. The
supernatant was discarded and the precipitate was re-suspended in 2.5 mL of re-
suspend solution containing 1x Ham's F12 Nutrient Mixture (Gibco), 1x DMEM,
Pen/Strep (100 units/mL and 100µg/mL respectively), and .1mg/mL DNase I (Roche).
The mixture was triturated 50 times with pipette to dissociate neurons and was then
passed through a 70 µm cell strainer (Falcon) into a 50 ml tube. 250 µl of FBS stock
was added to each sample and centrifuged for 5 minutes at 2000 rpm. The supernatant
was discarded and the precipitate was re-suspended in 3 mL of 1x Neurobasal medium
(NBM) (Gibco) supplemented with 1 mM sodium pyruvate (Gibco), Pen/Strep (100
units/mL and 100 µg/mL respectively), 2 mM L-Glutamine (Gibco), and 1x B-27
supplement (Gibco). The solution was then triturated 50 times with a pipette. Cell

density of the cell suspension was determined with the use of a hemacytometer (Hausser) with 10 μl of cell suspension and 10 μl trypan blue (Gibco) added. NBM was added as necessary to adjust cell density to 80-100 cells/mL. 1 mL of the cell suspension was added to each poly-L-lysine coated coverslip in individual wells of a 24-well plate. Cells were grown in an incubator at 37°C for 14 days until maturation with a quarter of the medium changed every 3-4 days.

GFP transfection and 7PA2 treatment of hippocampal culture

After 14 days of incubation, cells were prepared for GFP transfection with 1 mL of DMEM with 10% FBS and Pen/Strep added to each well 30-60 minutes before transfection. 1 μg DNA containing the GFP gene was mixed with 50 μl solution A (50 mM glucose in DMEM without FBS/Pen/Strep). 3 μl of Poly-Jet Reagent (SignaGen) was added to another 50 μl of solution A separate from the solution containing diluted DNA. The Poly-Jet solution was then immediately added to the diluted DNA solution and allowed to incubate at RT for 15 minutes. 100 μl of the solution was made for each well and added dropwise. The media was replaced after 5 hours with DMEM with 10% FBS and Pen/Strep.

Two days after the GFP transfection, primary hippocampal cultures were treated with 7PA2-CM with Aβ42 concentrations of 100, 150, or 250 pM for 2 hours. The media was then discarded and cultures were fixed with 4% paraformaldehyde (PFA) and 4% sucrose in 1x PBS for 15 minutes. 400 μl of the fixing solution was replaced after 15 minutes and cultures were fixed for an additional 15 minutes. The

cultures were then washed 3 times with 1x PBS (5 minutes each). Cultures were then coverslipped onto microscope slides (Fisherbrand). All neuronal cultures used in this study were prepared by Hiroko Maruyama.

Image acquisition and spine quantification in primary hippocampal cultures

Image acquisition was carried out on an Olympus DSU IX-81 inverted microscope fitted with a spinning disk confocal attachment and a 60x/1.2 N.A. water immersion objective. GFP labeled neurons were chosen randomly for imaging from neuronal cultures from two coverslips. For all dendritic spine analyses, segments selected for analysis had to fulfill the following three criteria: 1) the selected segment must be at least 50 μm away from the cell body; 2) the selected segment must be after the first branch point of the dendrite; and 3) the selected segment must not be at the ending tip of the dendrite. Additionally dendritic segments were selected such that no other segments overlapped with each other in a way that would obscure visualization of spines. Dendritic spine density was scored from three to five randomly chosen areas per neuron. Z-sections were taken at 0.3 μm intervals. All analyses were conducted blind to genotype. Spine counts for dendritic segments were acquired manually on Slidebook program with lengths of each dendritic segment measured on ImagePro 6.2.

RESULTS

D664A mutation does not affect dendritic spine density

In order to see if the DA mutation has any effect on dendritic spine density in mice, we first checked if there was any difference in neuronal dendritic spine density in brain sections between mice carrying the DA mutation and WT mice (Figure 5). In this section, "WT mouse" refers to GFP-M mouse and "DA mouse" refers to the DA/GFP-M mouse. GFP immunofluorescent staining was carried out using a chicken anti-GFP primary antibody and an AlexaFluor 488-conjugated donkey anti-chicken secondary antibody. DA and WT mice carrying one copy of the GFP transgene were selected for analysis due to difficulty in quantifying spines in microscope images of dendrites of mice carrying two copies of the GFP transgene. Our results showed that there was no significant difference between spine density of WT (average±SEM = 1.58±0.05 spines/μm) and DA mice (1.52±0.05 spines/μm) (p=0.60, Wilcoxon Rank Sum test), as assessed by manual acquisition of dendritic spine density from GFP immunofluorescent stained brain sections of 6 months to 12 months old mice (Figure 6).

To see if age has any effect on the dendritic spine density of DA and WT mice, the two genotypes were also compared against each other according to their age groups at either 6 months or 12 months (Figure 7). At both age groups there was no significant difference in spine density between WT and DA mice (6-month: 1.59±0.04 vs 1.56±0.08 spines/μm, p=0.93, Wilcoxcon Rank Sum test; 12-month: 1.56±014 vs

1.46±0.06 spines/μm, p=0.66, Wilcoxcon Rank Sum test). There was however a slight

decrease in spine density from 6 months old mice to 12 months old mice of both

genotypes but it did not reach statistical significance (p=0.90 for the WT group and

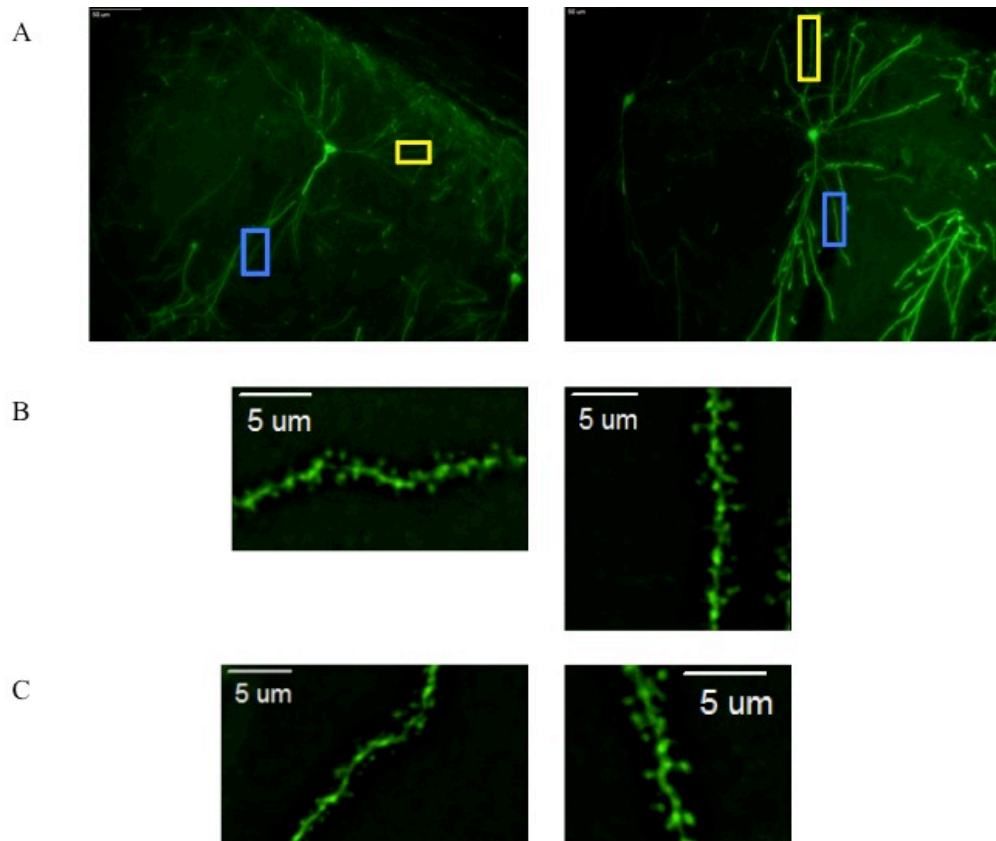p=0.65 for the DA group, Wilcoxon Rank Sum test).

Figure 5. Immunofluorescent images of GFP hippocampal neurons in DA/GFP-M mouse

WT/GFP-M neuron is shown in 5A on the left while DA/GFP-M neuron is shown on the right, both at 20x magnification. Basal dendritic segments in yellow boxes are enlarged in 5B at 60x magnification with optical zoom while apical dendritic segments in blue boxes are enlarged in 5C with the same magnification.
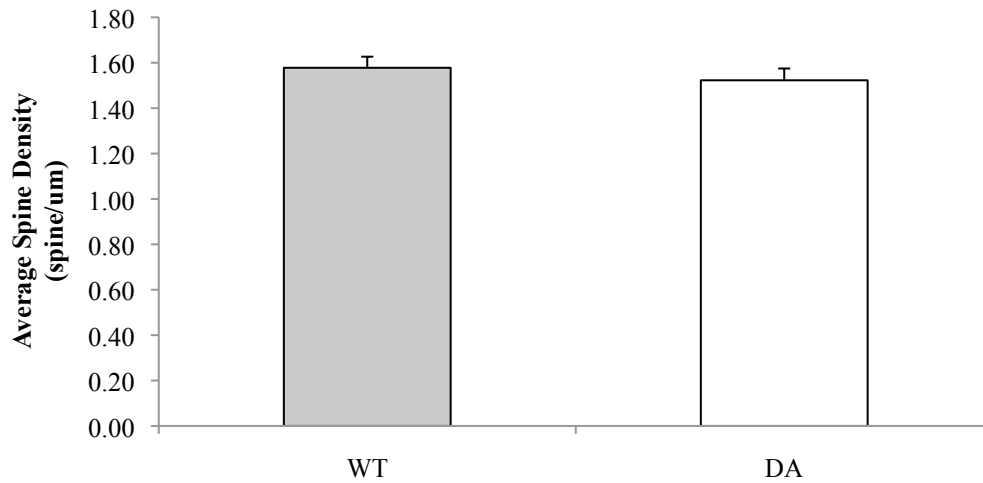
Figure 6: Dendritic spine density levels are similar between DA/GFP-M mice and WT/GFP-M mice

Dendritic spine density levels from CA1 neurons in 6-12 months old DA/GFP-M mice (n=8) and WT/GFP-M (n=9) mice expressed as mean ± SEM.
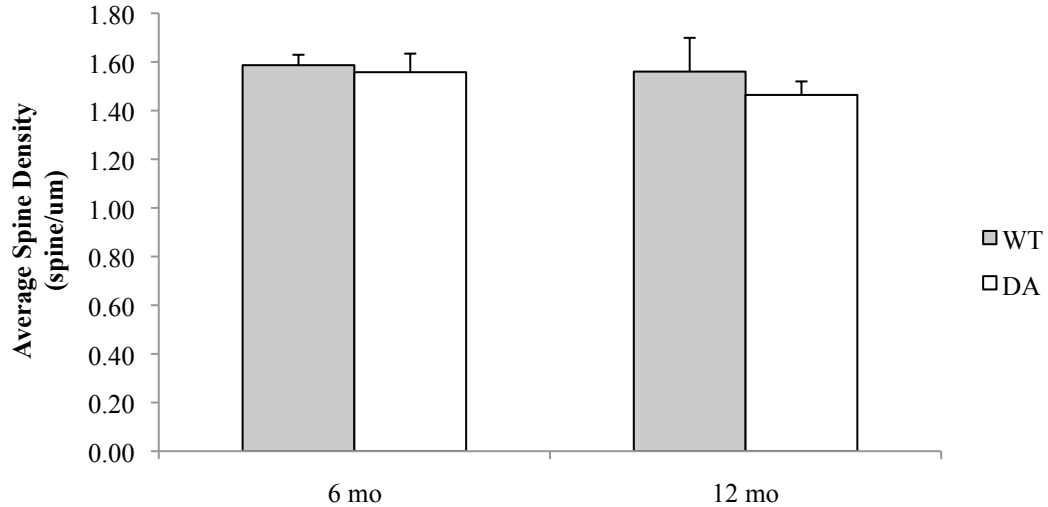

Figure 7: Dendritic spine density levels are similar between young (6-month) and adult (12-month) DA/GFP-M mice

Dendritic spine density levels from CA1 neurons in DA/GFP-M at 6 months of age (n=5) and 12 months of age (n=3) compared against WT/GFP-M mice at 6 months of age (n=6) and 12 months of age (n=3) expressed as mean ± SEM.

To see if there was a difference in the allocation of spines between different types of dendrites in the two genotypes, the spine density of apical dendrites and basal dendrites were compared between and within genotypes (Figure 8). No statistically significant difference was observed between basal or apical dendrites of DA and WT mice. We also compared apical and basal dendrites of WT and DA mice at different age groups at 6 months and 12 months of age (Figure 9). Similarly at 6 months of age there was no significant difference observed when comparing apical and basal dendrites of both genotypes. At 12 months of age there was a slight decrease observed in the spine density of apical and basal dendrites of DA mice that did not reach statistical significance. In summary the data suggested that this mutation does not alter spine density of adult DA mice.
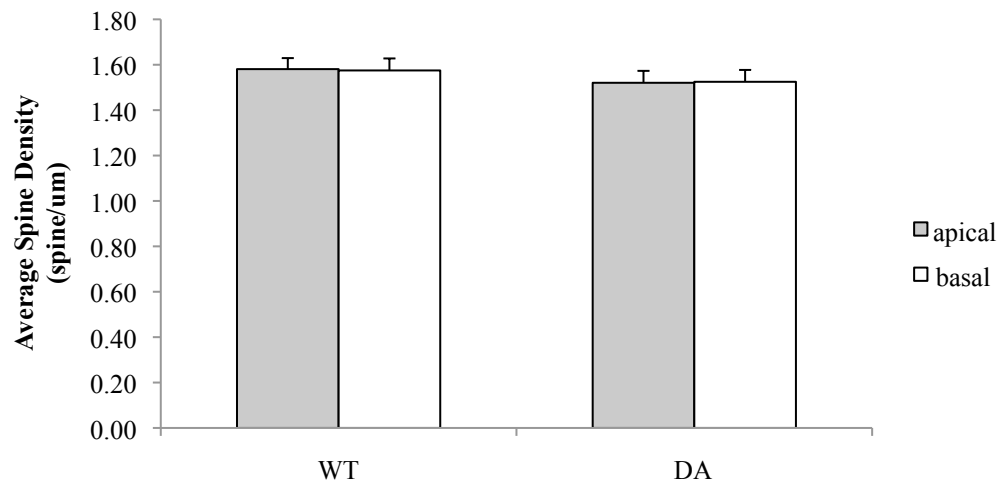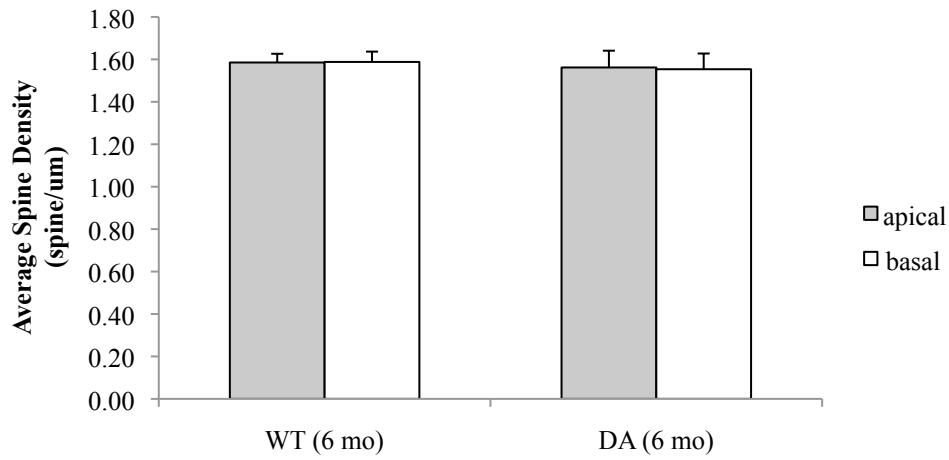
Figure 8. Apical and basal dendritic spine density levels are similar between DA/GFP-M mice

Comparison of apical and basal dendrites of CA1 neurons in 6-12 months old DA/GFP-M mice (n=8) and WT/GFP-M mice (n=9) in terms of dendritic spine density expressed as mean ± SEM.

A.

B.
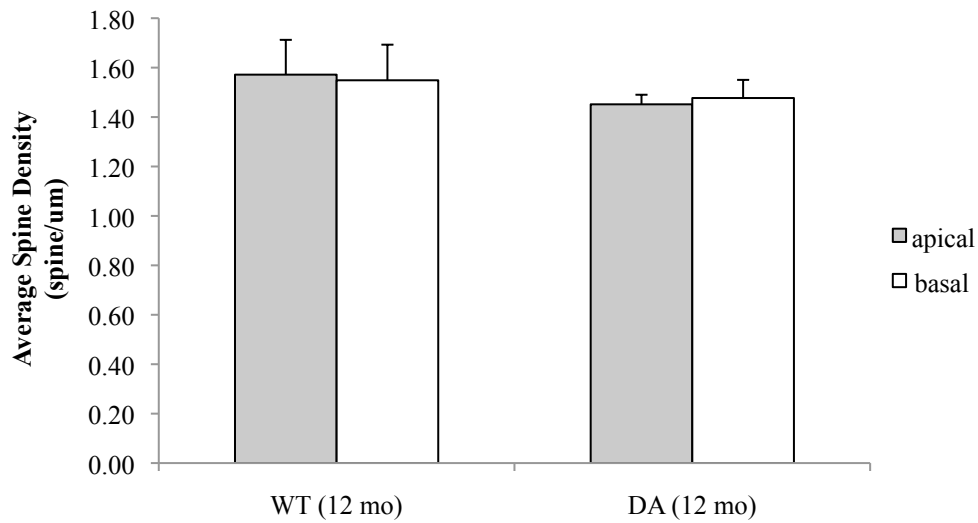

Figure 9. Apical and basal dendritic spine density levels are similar in DA/GFP-M mice across two different age groups

Comparison of apical and basal dendritic spine density of DA/GFP-M mice (n=5) and WT/GFP-M (n=6) mice at 6 months of age is shown in 9A. The same comparison is done at 12 months of age in 9B with DA/GFP-M mice (n=3) and WT/GFP-M mice (n=3). Both are expressed as mean ± SEM.

7PA2-CM without Aβ oligomers does not affect dendritic spine density

      To determine if the DA mutation can attenuate Aβ toxicity in DA mice, primary hippocampal neuronal cultures were prepared from P0-P1 pups of DA+/- parents. These cultures were then transiently transfected with GFP and treated with 7PA2-CM with varying concentrations of Aβ42 as analyzed by sandwich ELISA experiments probing for Aβ42 using MM26.2.1.3 antibody and HRP-conjugated 6E10 antibody (Figure 10). Aβ42 concentration of 7PA2-CM aliquots was adjusted from 780 pM in the original batch analyzed by ELISA experiments to 100 pM, 150 pM, and 250 pM with NBM for neuronal culture experiments. There was no significant difference observed between DA and WT cultures as assessed via manual acquisition of spine density from microscope images of dendrites regardless of the cultures being treated with Chinese Hamster Ovary (CHO) cell media or 7PA2-CM with varying concentrations of Aβ42 with the exception of WT neuronal cultures treated with CHO media and DA neuronal cultures treated with 250 pM 7PA2-CM (Figure 11). It was observed that there was a very slight trend in reduction in spine density in the DA cultures treated with 250 pM 7PA2-CM compared to WT cultures treated with CHO media.
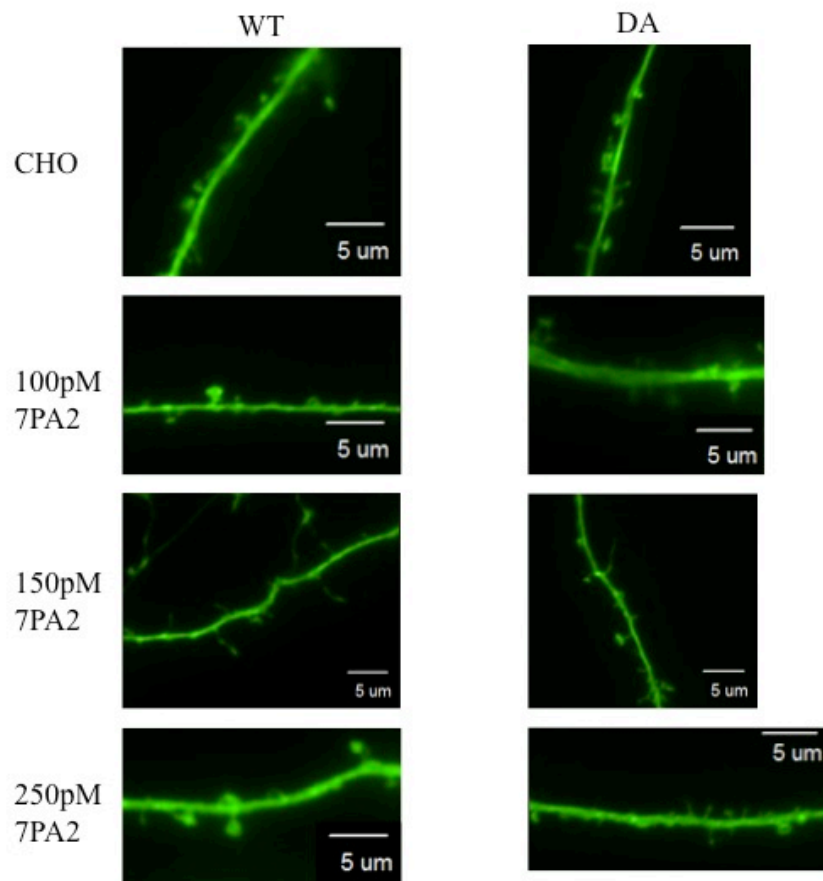
Figure 10. Representative images of primary hippocampal neuronal cultures from DA mice

Dendrites of neuronal cultures prepared from P0-P1 DA pups and WT littermates. Cultures were transiently transfected with GFP and treated with CHO or 7PA2-CM with varying concentrations of Aβ42. Images of dendritic segments were taken at 60x magnification with optical zoom.

Figure 11. Dendritic spine density levels of D664A and WT primary hippocampal neuronal cultures undergoing various Aβ42 treatments

DA and WT cultures were treated with either CHO media (n=7 and n=4 respectively), 100 pM 7PA2-CM (n=3 and n=3 respectively), 150 pM 7PA2-CM (n=2 and n=1 respectively), or 250 pM 7PA2-CM (n=4 and n=1 respectively). Dendritic spine density levels were expressed as mean ± SEM.

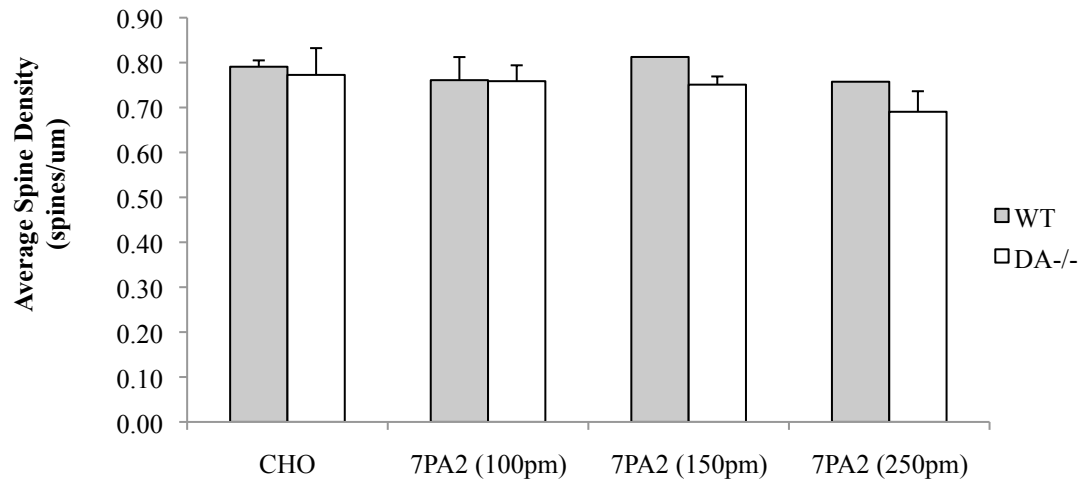Importantly, the WT cultures treated with Aβ-conditioned medium should have caused significant reduction in spine numbers seen by a number of laboratories and which we failed to replicate (Calabrese et al., 2007). Although ELISA experiments confirmed the presence of toxic Aβ42 peptides in the 7PA2-CM, toxic effects of the 7PA2-CM were not observed in the neuronal culture. Western blot experiments were therefore carried out to identify the various Aβ species in the 7PA2-CM used for neuronal culture experiments and it was revealed that the batch of 7PA2-CM collected for this study contained no Aβ oligomers (Figure 12). As previously demonstrated in other studies Aβ oligomers are required for 7PA2-CM to have toxic effects and decrease neuronal dendritic spine density levels (Shankar et al., 2007). The absence of oligomers in the batches of conditioned medium could explain the resistance of the neuronal cultures to synaptic injury. Further experiments with 7PA2-CM containing Aβ42 oligomers are needed to confirm that this is the reason for the lack of toxicity in the primary neuronal cultures treated with 7PA2-CM. If so, we can then test whether DA cultures demonstrated the predicted resistance to Aβ-induced synaptic toxicity.
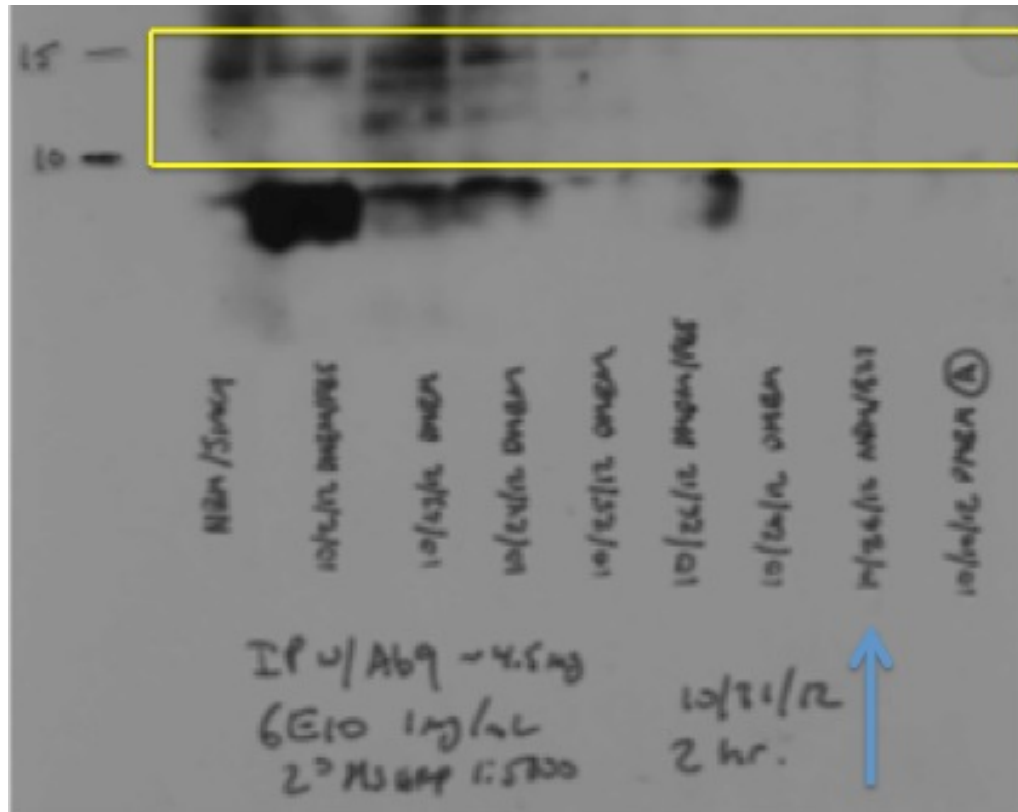
Figure 12. Western blot experiments probing for various Aβ species in 7PA2-conditioned medium

Batch 10/26/12 NBM/B27 (lane second from right) was used for neuronal culture experiments and it is seen that the batch lacks bands between 10-15 kDa indicating it contains no Aβ oligomers.

DISCUSSION

Our first aim was to examine whether the DA mutation had an effect on spine morphology of the DA mice compared to their WT littermates. Previous studies have shown that the DA mutation has a protective effect *in vivo* on mice overexpressing APP from behavioral abnormalities and could attenuate Aβ toxicity *in vitro* (Saganich et al., 2006, Zhang et al., 2010, Lu et al., 2000, 2003, Galvan et al., 2006). However, in these studies the mouse models used had other alterations accompanying them such as APP overexpression, making it difficult to quantify the protective effect contributed by the DA mutation. It was also unsure if the DA mutation prevented dendritic spine loss from Aβ treatment or APP overexpression or if the DA mutation increased initial levels of dendritic spine density, which would then be lowered by Aβ treatment or APP overxpression. By analyzing the spine density of the DA/GFP-M mouse line without any other alteration on APP apart from the DA mutation, we were able to confirm that the DA mutation has no effect on dendritic spine density when compared to WT mice.

DA mice and WT mice were compared against each other at different age groups – 6 months and 12 months of age. There were no significant differences observed in dendritic spine density between the two genotypes at either age group. Also, the spine density of apical and basal dendrites of both DA and WT mice were independently analyzed to see if the DA mutation had any effect on the allocation of spines across different parts of dendrites. Similarly, there was no difference observed

41

in spine density between apical and basal dendrites of both DA and WT mice. These results combined with overall dendritic spine density of the two genotypes indicate that the DA mutation has no effect on spine morphology of DA mice.

However, there is one drawback to using the DA/GFP-M mice to analyze the effects of the DA mutation on hippocampal neuronal dendritic spine morphology. The DA/GFP-M line was initially developed to be able to carry out experiments in a mouse line that's only alteration is the DA mutation, but our mouse line is also carrying the GFP transgene. The GFP transgene could potentially have had an effect on the spine morphology observed. However, since our results were negative and it was observed that the DA/GFP-M mice had no significant difference from the WT/GFP-M mice in terms of hippocampal dendritic spine morphology, it is not likely that the GFP transgene had any relevant impact on spine morphology or the alteration is uniform between DA/GFP-M mice and WT/GFP-M mice.

In future experiments we can further analyze the effects of the DA mutation on mice brain morphology by observing other traits of dendrite morphology such as dendrite arborization and comparing these traits between DA and WT mice. We can also repeat dendritic spine analysis in mice that are older than 12 months and even observe different subsets of neurons apart from the CA1 neurons described in this study. Eventually we can test the protective effects of the DA mutation to attenuate $A\beta$ toxicity *in vivo* in the DA mice by injecting $A\beta$ directly into the brains of mice or inserting genetic constructs such as the BRI-$A\beta$42 construct described by McGowan et al (2005) to have $A\beta$42 expressed in the brain.

Next we wanted to see if the DA mutation could attenuate Aβ toxicity in primary hippocampal neuronal cultures prepared from DA/GFP-M pups. It was observed that both WT and DA neuronal cultures had near identical spine densities regardless of whether they were treated with 7PA2-CM or CHO media. There was also no difference observed between neurons treated with different dilutions of 7PA2-CM with different concentrations of Aβ42. This result was not consistent with results from previous *in vitro* experiments where it was observed that primary hippocampal neuronal cultures had significantly lower dendritic spine density compared to control neurons when treated with 7PA2-CM containing Aβ oligomers (Calabrese et al., 2007). Our results indicate that the 7PA2-CM treatment had no effect on spine density of either genotype and that the lack of loss of spine in the DA neuronal culture cannot be attributed to the protective effects of the DA mutation. It was also observed that some groups had n-values that were too low for meaningful comparison with other groups. This was partially caused by loss of GFP signal from the neuronal cultures compared to when they were initially transiently transfected with GFP.

Retrospective western blot experiments were carried out on the 7PA2-CM batch used for the neuronal culture experiments and it was observed that the batch used contained minimal Aβ oligomers as we had initially assumed they would have. This would explain the results of the neuronal culture experiments and be consistent with results from Shankar et al (2007) in which it was reported that soluble low-n Aβ oligomers are required to observe the neurotoxic effects of Aβ treatment.

In conclusion, the dendritic spine density analyses of DA/GFP-M mice were successful and will serve as a negative control for future experiments indicating that the DA mutation itself has no effect on dendritic spine morphology of mice. The neuronal culture experiments need to be repeated perhaps with more samples as it was observed that many of the cultures lost their GFP signals over time after transient transfection. In future experiments involving the use of 7PA2-CM for Aβ treatment, it should be confirmed that the batch of 7PA2-CM used for these experiments show presence of Aβ oligomers in Western blot gels before they are used for the Aβ treatment of neuronal cultures. If the expected protective effects of the DA mutation can be observed in future hippocampal neuronal culture experiments with 7PA2-CM treatment with Aβ42 oligomers, then similar experiments can be carried out on organotypic slice cultures (OTSC) of DA mice as OTSC better resembles *in vivo* conditions compared to primary hippocampal neuronal cultures and give us further insight on the protective effects of the DA mutation from Aβ toxicity.

REFERENCES

Allinquant, B., Hantraye, P., Mailleux, P., Moya, K., Bouillot, C., and Prochiantz, A. (1995). Downregulation of amyloid precursor protein inhibits neurite outgrowth in vitro. J Cell Biol. *128(5),* 919-927.

Alzheimer's Association. (2014). 2014 Alzheimer's Disease Facts and Figures. Alzheimer's & Dementia. *10*, 1-75.

Baek S.H., Ohgi K.A., Rose D.W., Koo E.H., Glass C.K. and Rosenfeld M.G. (2002). Exchange of NCoR corepressor and Tip60 coactivator complexes links gene expression by NF-jB and b-amyloid precursor protein. Cell. *110*, 55–67.

Blennow, K., de Leon, M.J., and Zetterberg, H. (2006). Alzheimer's disease. Lancet. *368*, 387-403.

Calabrese, B., Shaked, G.M., Tabarean, I.V., Braga, J., Koo, E.H., and Halpain, S. (2007). Rapid, Concurrent Alterations in Pre- and Postsynaptic Structure Induced by Soluble Natural Amyloid-β Protein. Mol Cell Neurosci. *35(2),* 183-193.

Cao X., and Sudhof T. C. (2001). A transcriptionally active complex of APP with Fe65 and histone acetyltransferase Tip60. Science. *293*, 115–120.

Chen, J., Lin, K., and Chen, Y. (2009). Risk Factors for Dementia. J Formos Med Assoc. *108*, 754-764.

Corder, E.H., Saunders, A.M., Strittmatter, W.J., Schmechel, D.E., Gaskell, P.C., Small, G.W., Roses, A.D., Haines, J.L., and Pericak-Vance, M.A. (1993). Gene dose of apolipoprotein E type 4 allele and the risk of Alzheimer's disease in late onset families. Science. *261*, 921-923.

Galvan, V., Gorostiza, O.F., Banwait, S., Ataie, M., Logvinova, A.V., Sitaraman, S., Carlson, E., Sagi, S.A., Chevallier, N., Jin, K., Greenberg, D.A., and Bredesen, D.E. (2006). Reversal of Alzheimer's-like pathology and behavior in human APP transgenic mice by mutation of Asp664. Proc Natl Acad Sci U S A. *103(18),* 7130-7135.

Glenner, G.G., and Wong, C.W. (1984). Alzheimer's disease: initial report of the purification and characterization of a novel cerebrovascular amyloid protein. Biochemical and Biophysical Research Communications. *120(3)*, 885-890.

Goate, A., Chartier-Harlin, M., Mullan, M., Brown, J., Crawford, F., Fidani, L., Giuffra, L., Haynes, A., Irving, N., James, L., Mant, R., Newton, P., Rooke, K., Roques, P., Talbot, C., Pericak-Vance, M., Roses, A., Williamson, R., Rossor, M., Owen, M., and Hardy, J. (1991). Segregation of mutation in the amyloid precursor protein gene with familial Alzheimer's disease. Nature. *349*, 704-706.

Goedert, M., Wischik, C.M., Crowther, R.A., Walker, J.E., and Klug, A. (1988). Cloning and sequencing of the cDNA encoding a core protein of the paired helical filament of Alzheimer disease: Identification as the microtubule-associated protein tau. Proc Natl Acad Sci USA. *85*, 4051-4055.

Goodman, Y., and Mattson, M.P. (1994). Secreted forms of beta-amyloid precursor protein protect hippocampal neurons against amyloid beta-peptide-induced oxidative injury. Experimental Neurology. *128(1)*, 1-12.

Hardy, J.A., and Higgins, G.A. (1992). Alzheimer's Disease: The Amyloid Cascade Hypothesis. Science. *256*, 184-185.

Hardy, J.A., and Selkoe, D.J. (2002). The amyloid hypothesis of Alzheimer's disease: progress and problems on the road to therapeutics. Science. *297(5580)*, 353-356. Harvey, R.J., Skelton-Robinson, M., and Rossor, M.N. (2003). The prevalence and causes of dementia in people under the age of 65 years. J Neurol Neurosurg Psychiatry. *74*, 1206-1209.

Harris, J.A., Devidze, N., Halabisky, B., Lo, I., Thwin, M.T., Yu, G., Bredesen, D.E., Masliah, E., and Mucke, L. (2010). Many Neuronal and Behavioral Impairments in Transgenic Mouse Models of Alzheimer's Disease Are Independent of Caspase Cleavage of the Amyloid Precursor Protein. N Neurosci. *30(1),* 372-381.

Hebert, L.E., Weuve, J., Scherr, P.A., and Evans, D.A. (2013). Alzheimer disease in the United States (2010-2050) estimated using the 2010 Census. Neurology. *80(19)*, 1778-1783.

Herard, A.S., Besret, L., Dubois, A., Dauguet, J., Delzescaux, T., Hantraye, P., Bonvento, G., and Moya, K.L. (2006). siRNA targeted against amyloid precursor protein impairs synaptic activity in vivo. Neurobiol Aging. *27(12),* 1740-1750.

Ho, A., and Sudhof, T.C. (2004). Binding of F-spondin to amyuloid-beta precursor protein: a candidate amyloid-beta precursor protein ligand that modulates amyloid-beta precursor protein cleavage. Proc Natl Acad Sci U S A. *101(8),* 2548-2553.

Iqbal, K., Alonso, A., Chen, S., Chohan, O.M., El-Akkad, E., Gong, C., Khatoon, S., Li, B., Liu, F., Rahman, A., Tanimukai, H., and Grundke-Iqbal, I. (2005). Tau pathology in Alzheimer disease and other tauopathies. Biochimica et biophysica acta. *1739*, 198-210.

Iwatsubo, T. (2004). The γ-secretase complex: machinery for intramembrane proteolysis. Curr Opin Neurobiol. *14(3)*, 379-383.

Jiang, Q., Lee, C.Y., Mandrekar, S., Wilkinson, B., Cramer, P., Zelcer, N., Mann, K., Lamb, B., Willson, T.M., Collins, J.L., Richardson, J.C., Smith J.D., Comery, T.A., Riddell D., Holtzman, D.M., Tontonoz, P., and Landreth, G.E. (2008). ApoE promotes the proteolytic degradation of Aβ. Neuron. *58(5)*, 681-693.

Kinoshita A., Whelan C.M., Berezovska O. and Hyman B.T. (2002). The c secretase-generated carboxyl-terminal domain of the amyloid precursor protein induces apoptosis via Tip60 in H4 cells. J. Biol. Chem. *277*, 28530–28536.

Lorenzo, A., Yuan, M., Zhang, Z., Paganetti, P.A., Sturchler-Pierrat, C., Staufenbiel, M., Mautino, J., Vigo, F.S., Sommer, B., and Yankner, B.A. (2000). Amyloid beta interacts with the amyloid precursor protein: a potential toxic mechanism in Alzheimer's disease. Nat Neurosci. *3(5),* 460-464.

Lourenco, F.C., Galvan, V., Fombonne, J., Corset, V., Llambi, F., Muller, U., Bredesen, D.E., and Mehlen, P. (2009). Netrin-1 interacts with amyloid precursor protein and regulates amyloid-beta production. Cell Death Differ. *16(5),* 655-663.

Lu, D.C., Rabizadeh, S., Chandra, S., Shayya, R.F., Ellerby, L.M., Ye, X., Salvesen, G.S., Koo, E.H., and Bredesen, D.E. (2000). A second cytotoxic proteolytic peptide derived from amyloid B-protein precursor. Nature Medicine. *6*, 397-404.

Lu, D.C., Soriano, S., Bredesen, D.E., and Koo, E.H. (2003). Caspase cleavage of the amyloid precursor protein modulates amyloid β-protein toxicity. Journal of Neurochemistry. *87*, 733-741.

Mayeux, R., Sano, M., Chen, J., Tatemichi, T., and Stern, Y. (1991). Risk of dementia in first-degree relatives of patients with Alzheimer's disease and related disorders. Archives of Neurology. *48*, 269-273.

McGowan, E., Pickford, F., Kim, J., Onstead, L., Eriksen, J., Yu, C., Skipper, L., Murphy, P.M., Beard, J., Das, P., Jansen, K., DeLucia, M., Lin, W., Dolios, G., Wang, R., Eckman, C.B., Dickson, D.W., Hutton, M., Hardy, J., and Golde, T. (2005). Aβ42 Is Essential for Parenchymal and Vascular Amyloid Deposition in Mice. Neuron. *47(2),* 191-199.

Midthune, B., Malinow, R., and Koo, E. (2011). Elimination of APP caspase cleavage site D664 attenuates Aβ-mediated synaptic depression. Alzheimer's & Dementia. *7(4),* S588.

Park, J.H., Gimbel, D.A., GrandPre, T., Lee, J.K., Kim, J.E., Li, W., Lee, D.H., and Strittmatter, S.M. (2006). Alzheimer precursor protein interaction with the Nogo-66 receptor reduces amyloid-beta plaque deposition. J Neurosci. *26(5),* 1386-1395.

Perez, R.G., Zheng, H., Van der Ploeg, L.H., and Koo, E.H. (1997). The beta-amyloid precursor protein of Alzheimer's disease enhances neuron viability and modulates neuronal polarity. J Neurosci. *17(24),* 9407-9414.

Price, J.L., McKeel, D.W., Buckles, V.D., Roe, C.M., Xiong, C., Grundman, M., Hansen, L.A., Petersen, R.C., Parisi, J.E., Dickson, D.W., Smith, C.D., Davis, D.G., Schmitt, F.A., Markesbery, W.R., Kaye, J., Kurlan, R., Hulette, C., Kurland, B.F., Higdon, R., Kukull, W., and Morris, J.C. (2009). Neuropathology of nondemented aging: Presumptive evidence for preclinical Alzheimer disease. Neurobiology of Aging. *30*, 1026-1036.

Purohit, D.P., Batheja, N.O., Sano, M., Jashnani, K.D., Kalaria, R.N., Karunamurthy, A., Kaur, S., Shenoy, A.S., Van Dyk, K., Schmeidler, J., and Perl D.P. (2011). Profiles of Alzheimer's disease-related pathology in an aging urban population sample in India. Journal of Alzheimer's Disease. *24(1)*, 187-196.

Saganich, M.J., Schroeder, B.E., Galvan, V., Bredesen, D.E., Koo, E.H., and Heinemann, S.F. (2006). Deficits in Synaptic Transmission and Learning in Amyloid Precursor Protein (APP) Transgenic Mice Require C-Terminal Cleavage of APP. The Journal of Neuroscience. *26(52)*, 13428-13436.

Selkoe, D.J. (2001). Alzheimer's disease: genes, proteins, and therapy. Physiol Rev. *81(2)*, 741-766.

Shankar, G.M., Bloodgood, B.L., Townsend, M., Walsh, D.M., Selkoe, D.J., and Sabatini, B.L. (2007). Natural Oligomers of the Alzheimer Amyloid-β Protein Induce Reversible Synapse Loss by Mediating an NMDA-Type Glutamate Receptor-Dependent Signaling Pathway. The Journal of Neuroscience. *27*, 2866-2875.

Sisodia, S.S., Koo, E.H., Hoffman, P.N., Perry, G., and Price, D.L. (1993). Identification and transport of full-length amyloid precursor proteins in rat peripheral nervous system. The Journal of Neuroscience. *13*, 3136-3142.

Soriano, S., Lu, D.C., Chandra, S., Pietrzik, C.U., and Koo, E.H. (2001). The Amyloidogenic Pathway of Amyloid Precursor Protein (APP) Is Independent of Its Cleavage by Caspases. The Journal of Biological Chemistry. *276,* 29045-29050.

Strittmatter, W.J., Saunders A.M., Schmechel, D., Pericak-Vance, M., Enghild, J., Salvesen, G.S., and Roses, A.D. (1993). Apolipoprotein E: high-avidity binding to beta-amyloid and increased frequency of type 4 allele in late-onset familial Alzheimer disease. Proc Natl Acad Sci USA. *90*, 1977-1981.

Tanzi, R.E., and Bertram, L. (2005). Twenty years of the Alzheimer's disease amyloid hypothesis: a genetic perspective. Cell. *120(4)*, 545-555.

Taylor, C.J., Ireland, D.R., Ballagh, I., Bourne, K., Marechal, N.M., Turner, P.R., Bilkey, D.K., Tate, W.P., and Abraham, W.C. Endogenous secreted amyloid precursor protein-alpha regulates hippocampal NMDA receptor function, long-term potentiation and spatial memory. Neurobiol Dis. *31(2),* 250-260.

Wang, J., Xia, Y., Grundke-Iqbal, I., and Iqbal, K. (2013). Abnormal Hyperphosphorylation of Tau: Sites, Regulation, and Molecular Mechanism of Neurofibrillary Degeneration. Journal of Alzheimer's Disease. *33*, 123-139.

Weidemann, A., Paliga, K., Durrwang, U., Reinhard, F.B.M., Schuckert, O., Evin, G., and Masters, C.L. (1999). Proteolytic Processing of the Alzheimer's Disease Amyloid Precursor Protein within Its Cytoplasmic Domain by Caspase-like Proteases. The Journal of Biological Chemistry. *274*, 5823-5829.

Yaffe, K., Barnes, D., Nevitt, M., Lui, L.Y., and Covinsky, K. (2001). A prospective study of physical activity and cognitive decline in elderly women: women who walk. Arch Intern Med. *161*, 1703-1708.

Zhang, J., Gorostiza, O.F., Tang, H., Bredesen, D.E., and Galvan, V. (2010). Reversal of learning deficits in hAPP transgenic mice carrying a mutation at Asp664: A role for early experience. Behavioural Brain Research. *206*, 202-207.

Zheng, H., and Koo, E.H. (2011). Biology and pathophysiology of the amyloid precursor protein. Molecular Neurodegeneration. *6*, 1-16.